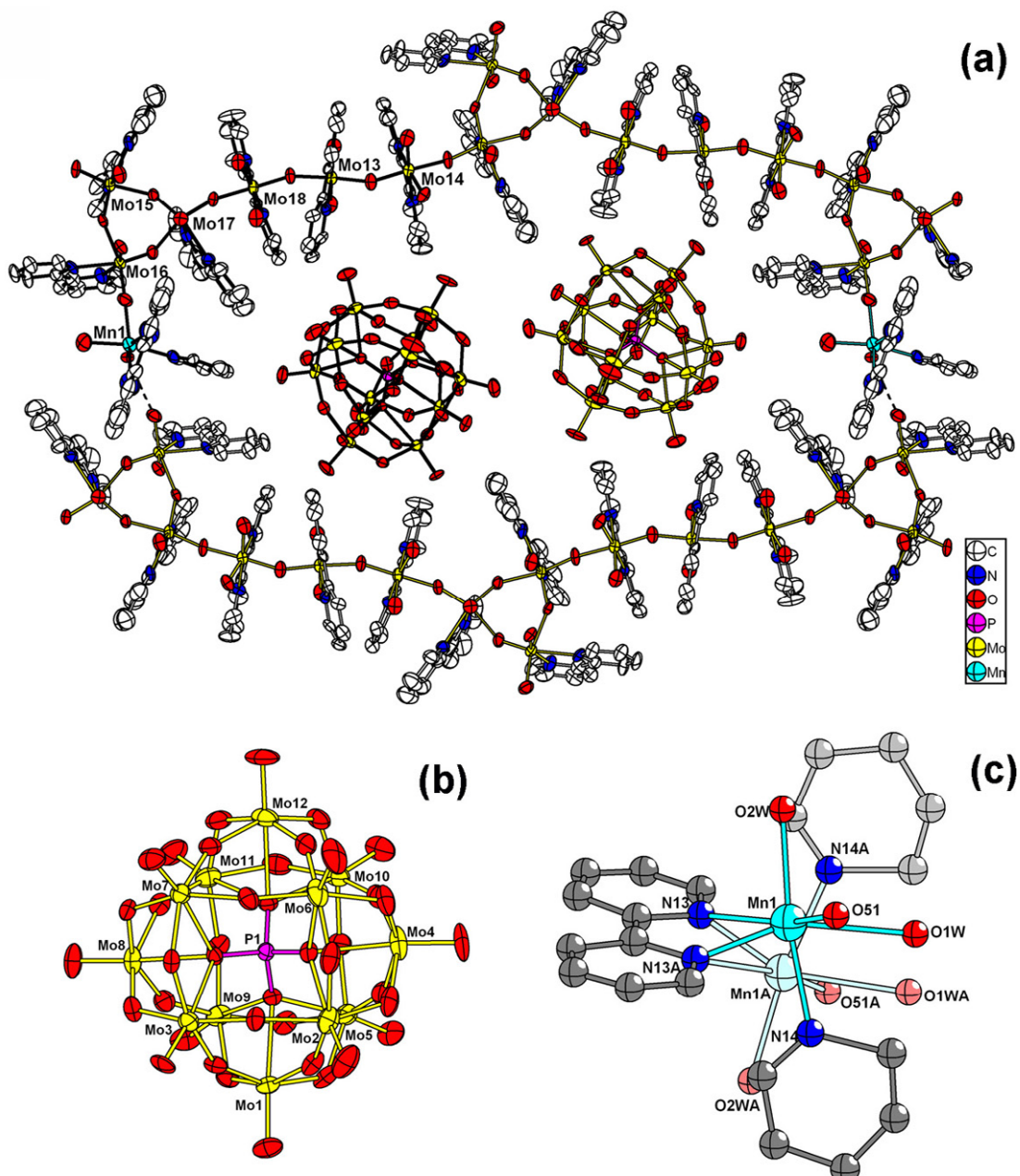
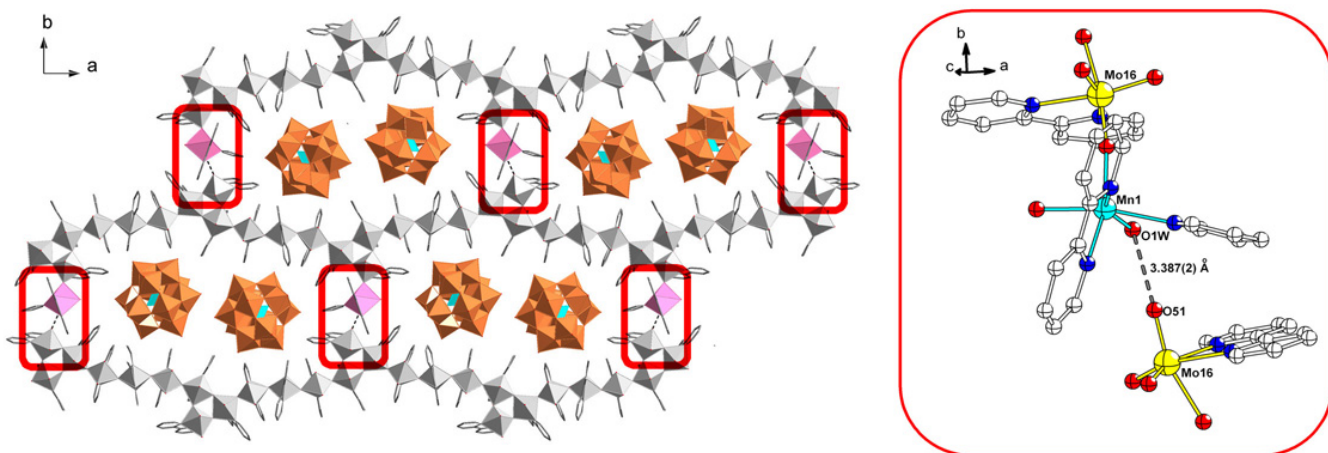


## A new molybdenum-oxide-based organic-inorganic hybrid framework templated by double Keggin anions

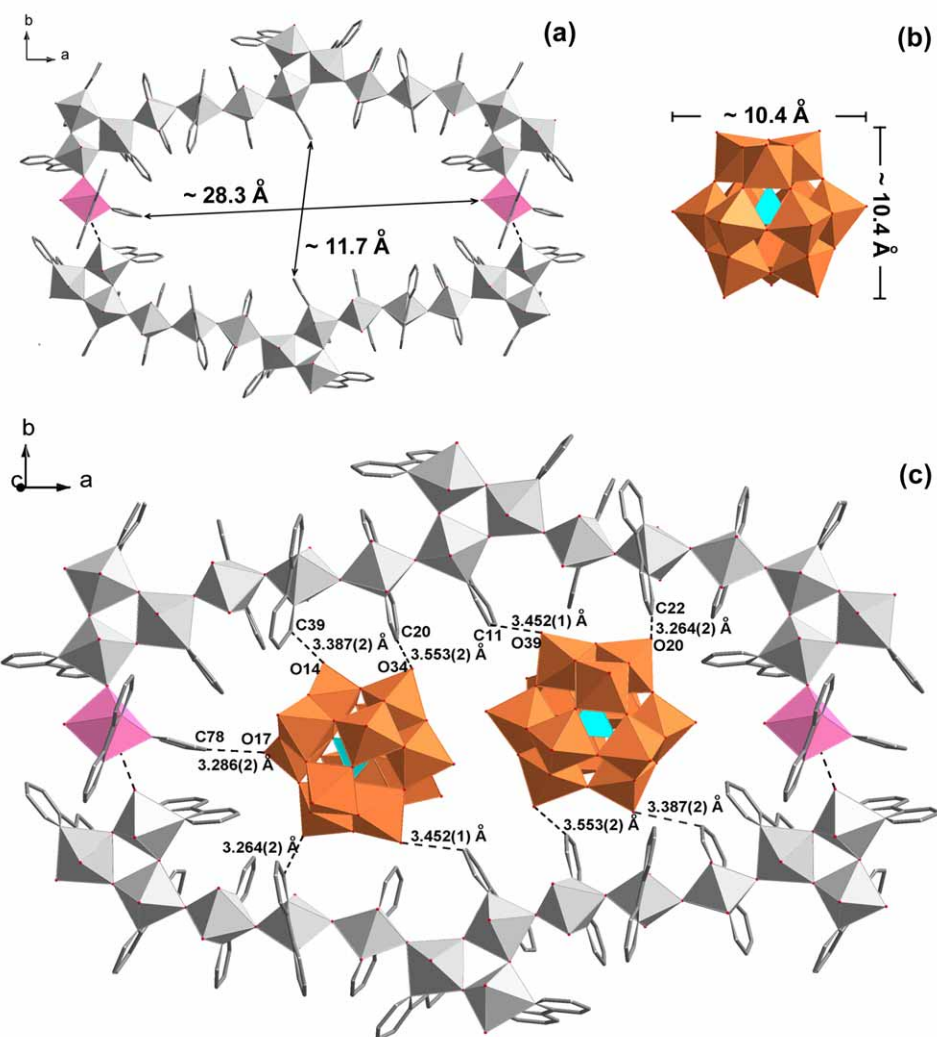
Yang-Guang Li,<sup>a</sup> Li-Mei Dai,<sup>a,b</sup> Yong-Hui Wang,<sup>a</sup> Xin-Long Wang,<sup>a</sup> En-Bo Wang,<sup>a,\*</sup> Zhong-Min Su<sup>a,\*</sup> and Lin Xu<sup>a</sup>



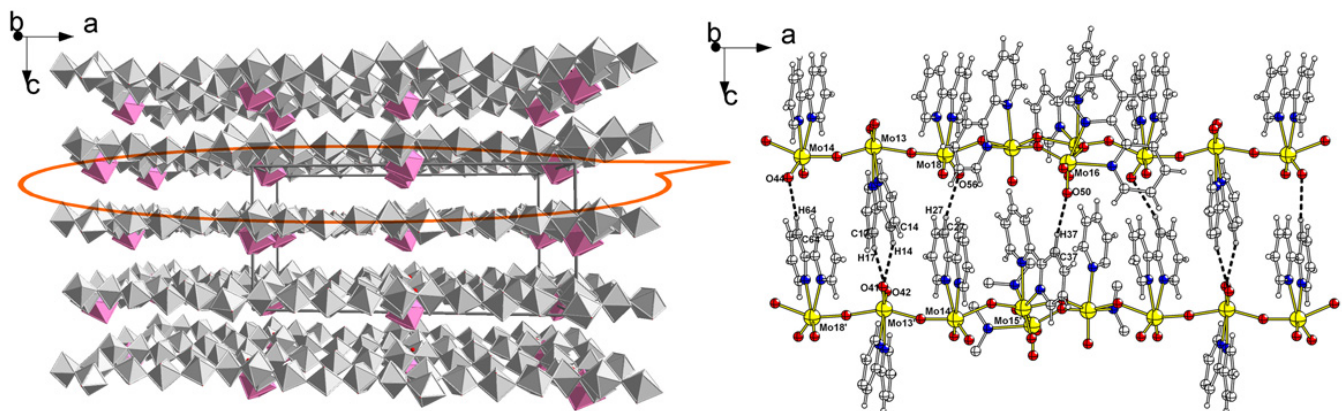
**Fig. S1** (a) ORTEP plot of **1** with 30% thermal ellipsoids. The H atoms and the solvent water molecules are omitted for clarity. The asymmetric unit in the cell is emphasized with black bonds; (b) ORTEP plot of the  $\alpha$ -Keggin polyanion  $[PMo_{12}O_{40}]^{3-}$  in **1** (30% thermal ellipsoids); (c) The ball-and-stick view of the  $[Mn(bpy)(py)(H_2O)_2]^{2+}$  unit disordered into two positions with 50% occupancies, respectively.



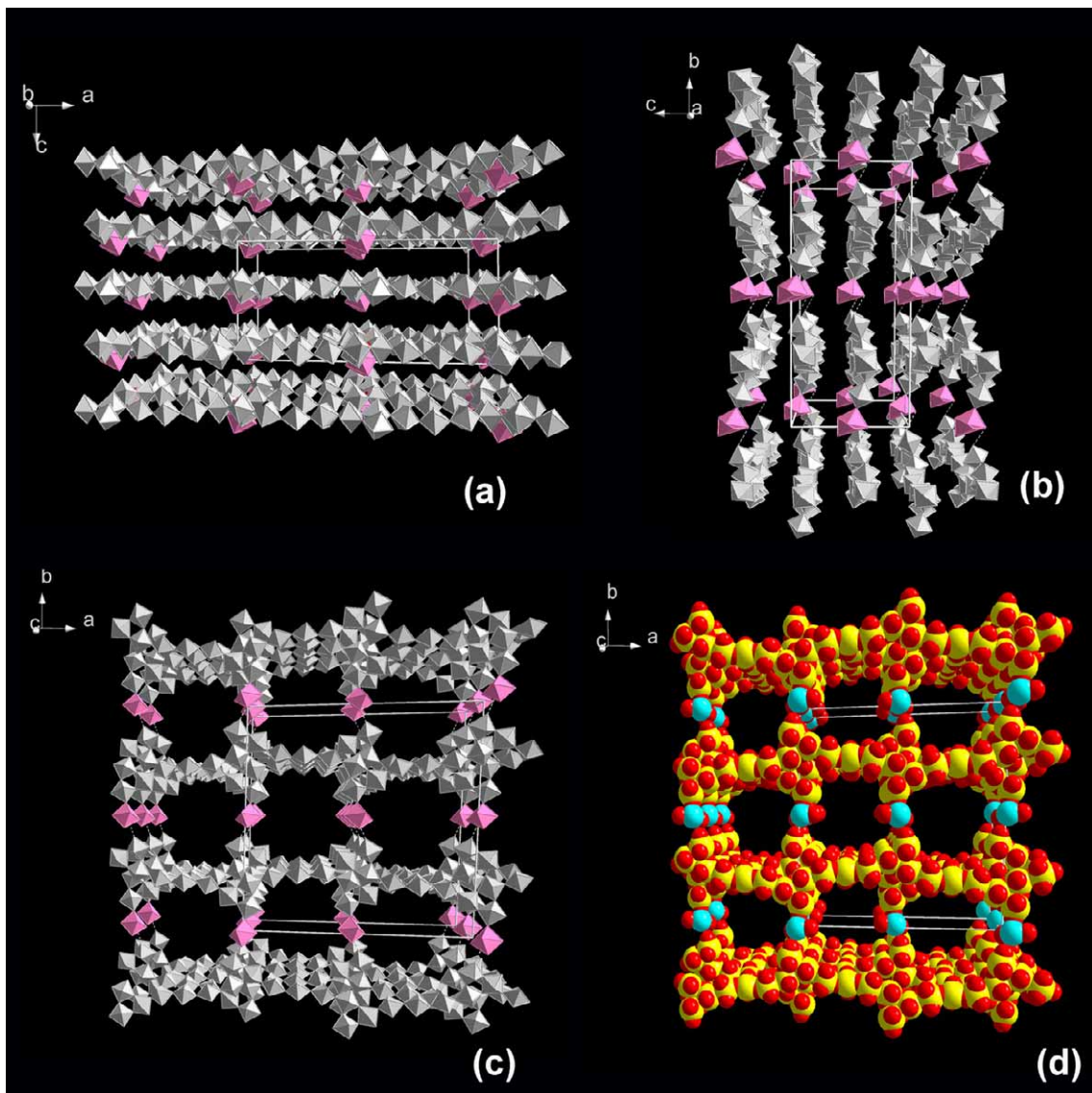
**Fig. S2** View of the H-bonds between O1W of the  $[\text{Mn}(\text{bpy})(\text{py})(\text{H}_2\text{O})_2]^{2+}$  unit and terminal oxygen atom O51 of the adjacent hybrid molybdenum oxide layer. The distance of O1W...O51 3.387(2) Å. Based on this H-bond, the infinite hybrid chains are connected into 2-D supramolecular layer on the *ab* plane or [001] plane.



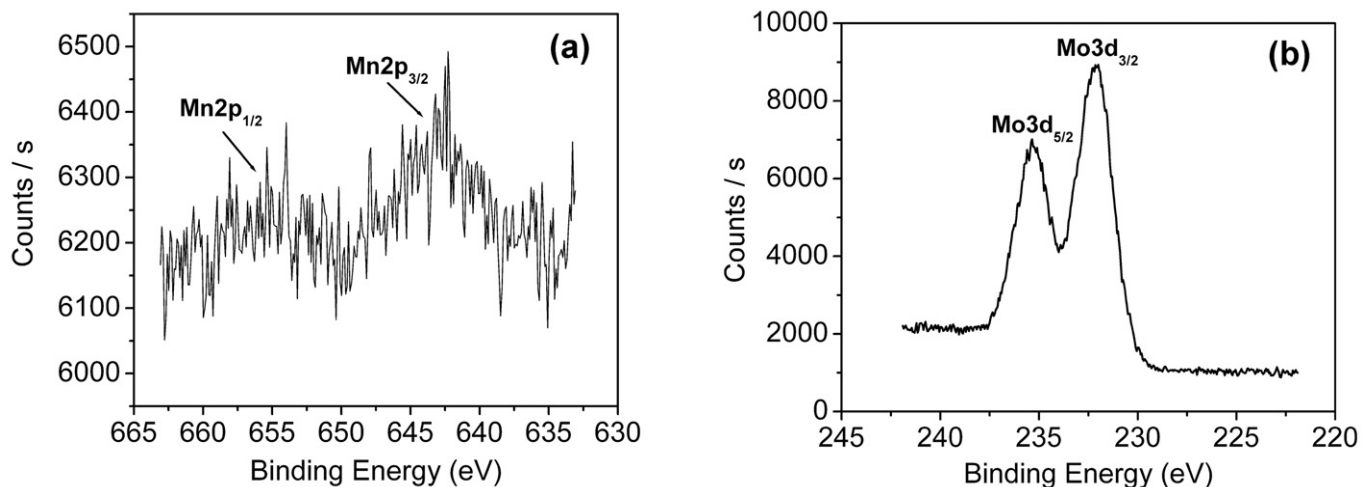
**Fig. S3** (a) View of the pore size of 2-D supramolecular network “host” in **1**, the pore size is dependent on the distance between C78 derived from py ligand and O2W on the Mn centers, and the distance of C38 of bpy ligands and its symmetric operation (C38A); (b) View of the size of the Keggin polyanion; (c) View of the H-bonds between the surface of Keggin-ions and inner surface of the composite host.



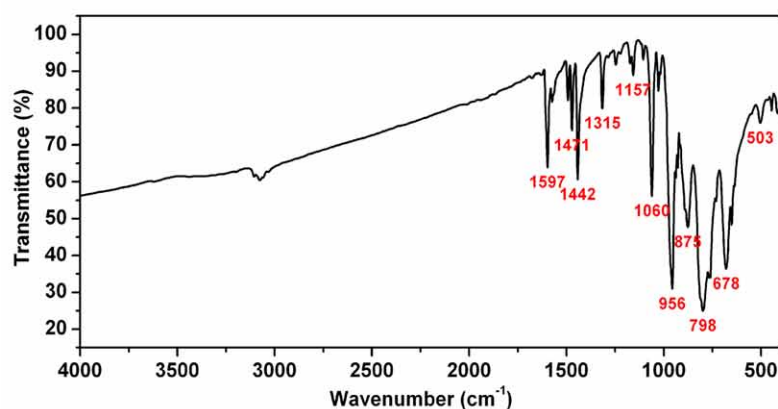
**Fig. S4** View of the extensive H-bonds between C-H groups of bpy ligands and oxygen atoms of neighbouring hybrid metal oxide layer. The typical H-bonds are shown in Table S3.



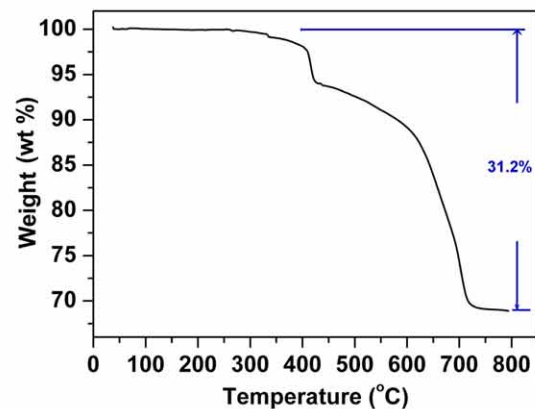
**Fig. S5** View of the packing arrangements of hybrid molybdenum-oxide scaffolding hosts in **1** (a) along *b* axis; (b) along *a* axis; (c) along *c* axis. The organic ligands and Keggin ion templates are omitted for clarity. (d) Space-filling diagram showing the 3-D hybrid metal oxide host in **1**.



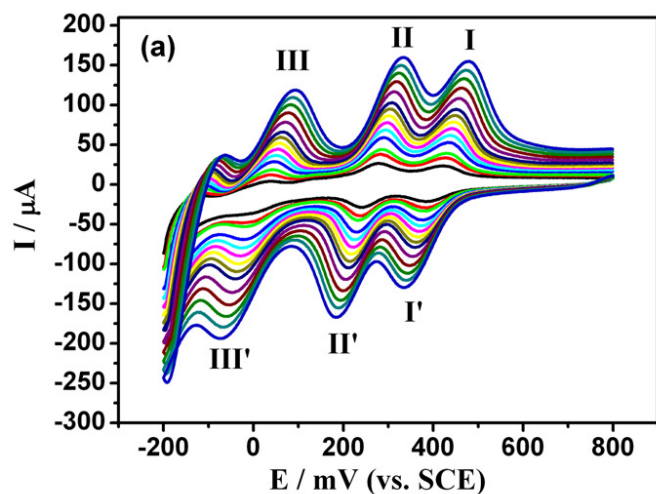
**Fig. S6** The XPS spectra of compound **1** for (a) Mn<sup>2+</sup> and (b) Mo<sup>6+</sup>.



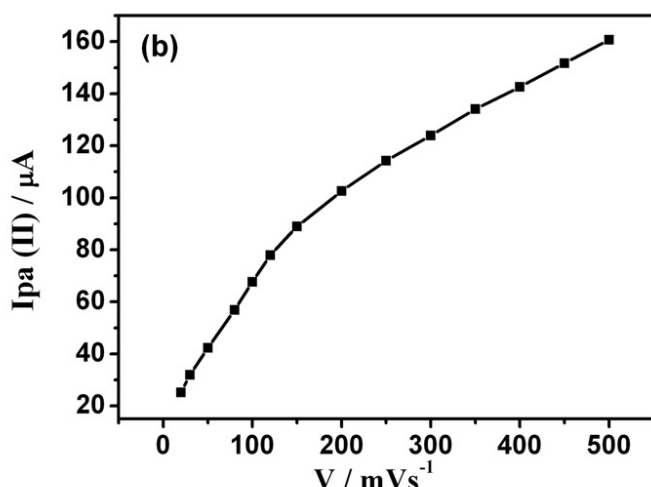
**Fig. S7** The IR spectrum of **1**.



**Fig. S8** The TG curve of **1**.



**Fig. S9** a) Cyclic voltammograms of the **1**-CPE in the 1 M H₂SO₄ solution at different scan rates (from inner to outer: 20, 30, 50, 80, 100, 120, 150, 200, 250, 300, 350, 400, 450, 500 mV s<sup>-1</sup>). Potentials vs. SCE; The CV of **1**-CPE shows three reversible redox peaks in the potential range +700 to -100 mV. The mean peak potentials E<sub>1/2</sub>=(E<sub>pa</sub>+E<sub>pc</sub>)/2 are +397, +251 and +6 mV, respectively (based on the CV at 50 mV s<sup>-1</sup>). The redox peaks I-I', II-II' and III-III' correspond to reduction and re-oxidation of [PMo<sub>12</sub>O<sub>40</sub>]<sup>3-</sup> in **1** through two-, four- and six-electron process, respectively. b) The dependence of anodic peak II current on scan rates. At scan rates lower than 120 mV s<sup>-1</sup>, the peak currents were proportional to the scan rate, indicating that the redox process of the **1**-CPE is surface-controlled; while at scan rates higher than 120 mV s<sup>-1</sup>, the peak currents were proportional to the square root of the scan rate, suggesting that redox process of the **1**-CPE is diffusion-controlled.



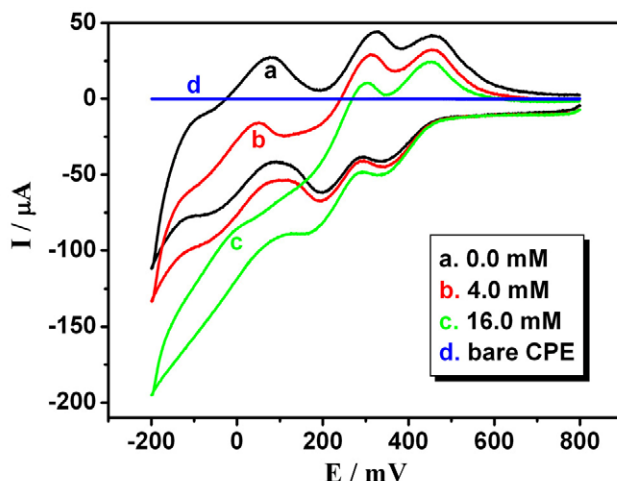


**Fig. S10** Cyclic voltammograms of the **1**-CPE in 1 M  $\text{H}_2\text{SO}_4$  solution containing 0.0, 4.0, 16.0 mM  $\text{NaNO}_2$  and a bare CPE in 5.0 mM  $\text{NaNO}_2$  + 1 M  $\text{H}_2\text{SO}_4$  solution. Potentials vs. SCE. Scan rate: 50 mV s<sup>-1</sup>.

**Table S1** Crystal data and structure refinement for **1**

Empirical formula	$\text{C}_{135}\text{H}_{117}\text{N}_{27}\text{O}_{118}\text{P}_2\text{MnMo}_{36}$
Formula weight	7576.28
Temperature	293(2) K
Wavelength (Å)	0.71073
Crystal system	Orthorhombic
Space group	Aba2
a (Å)	34.826(7)
b (Å)	35.777(7)
c (Å)	16.575(3)
$\alpha$ (°)	90
$\beta$ (°)	90
$\gamma$ (°)	90
V (Å <sup>3</sup> )	20652(7)
Z	4
Calculated density (Mg/m <sup>3</sup> )	2.437
Absorption coefficient (mm <sup>-1</sup> )	2.282
F(000)	14508
Crystal size (mm)	0.29 × 0.27 × 0.23
Theta range for data collection (°)	3.14 ≤ θ ≤ 25.00
Limiting indices	-41 ≤ h ≤ 40, -42 ≤ k ≤ 42, -19 ≤ l ≤ 19
Reflections collected / unique	73762 / 18161 [R(int) = 0.1164]
Max. and min. transmission	0.6219 and 0.5574
Goodness-of-fit on $F^2$	0.872
Final R indices [ $I > 2 \sigma(I)$ ] <sup>a</sup>	$R_1 = 0.0465, wR_2 = 0.0869$
R indices (all data) <sup>b</sup>	$R_1 = 0.0691, wR_2 = 0.0943$
Absolute structure parameter	-0.04(3)
Largest diff. peak and hole (eÅ <sup>-3</sup> )	1.018 and -0.681

<sup>a</sup>  $R_1 = \sum ||F_0| - |F_c|| / \sum |F_0|$ ; <sup>b</sup>  $wR_2 = \sqrt{[w(F_0^2 - F_c^2)^2] / \sum [w(F_0^2)^2]}^{1/2}$

**Table S2** Selected Bond lengths [Å] and angles [°] for **1**.

Mo(1)-O(8)	1.668(7)	Mo(2)-O(13)	1.669(7)
Mo(1)-O(9)	1.873(7)	Mo(2)-O(11)	1.869(8)
Mo(1)-O(5)	1.877(6)	Mo(2)-O(6)	1.907(7)
Mo(1)-O(6)	1.924(7)	Mo(2)-O(10)	1.955(7)
Mo(1)-O(7)	1.965(8)	Mo(2)-O(12)	1.956(8)
Mo(1)-O(3)	2.432(6)	Mo(2)-O(2)	2.436(7)
Mo(3)-O(14)	1.676(7)	Mo(4)-O(20)	1.675(8)
Mo(3)-O(10)	1.880(7)	Mo(4)-O(19)	1.850(8)
Mo(3)-O(15)	1.883(7)	Mo(4)-O(21)	1.885(7)
Mo(3)-O(16)	1.953(6)	Mo(4)-O(11)	1.982(8)
Mo(3)-O(9)	1.955(7)	Mo(4)-O(18)	1.998(8)
Mo(3)-O(1)	2.429(6)	Mo(4)-O(2)	2.434(7)
Mo(5)-O(24)	1.682(7)	Mo(6)-O(28)	1.680(8)
Mo(5)-O(18)	1.830(8)	Mo(6)-O(25)	1.848(7)
Mo(5)-O(7)	1.897(8)	Mo(6)-O(12)	1.891(8)
Mo(5)-O(22)	1.952(7)	Mo(6)-O(26)	1.942(8)
Mo(5)-O(23)	2.013(7)	Mo(6)-O(19)	2.011(9)
Mo(5)-O(3)	2.424(7)	Mo(6)-O(2)	2.421(6)
Mo(7)-O(30)	1.677(7)	Mo(8)-O(34)	1.661(8)
Mo(7)-O(31)	1.863(7)	Mo(8)-O(33)	1.850(7)
Mo(7)-O(29)	1.872(8)	Mo(8)-O(16)	1.883(6)
Mo(7)-O(25)	1.957(7)	Mo(8)-O(32)	1.949(8)
Mo(7)-O(15)	1.972(7)	Mo(8)-O(31)	1.996(7)
Mo(7)-O(1)	2.446(7)	Mo(8)-O(1)	2.421(6)
Mo(9)-O(35)	1.667(8)	Mo(10)-O(39)	1.675(8)
Mo(9)-O(23)	1.872(8)	Mo(10)-O(22)	1.876(7)
Mo(9)-O(36)	1.879(7)	Mo(10)-O(38)	1.883(8)
Mo(9)-O(5)	1.954(6)	Mo(10)-O(37)	1.934(7)
Mo(9)-O(33)	1.965(8)	Mo(10)-O(21)	1.947(7)
Mo(9)-O(3)	2.432(6)	Mo(10)-O(4)	2.442(7)
Mo(11)-O(17)	1.671(7)	Mo(12)-O(27)	1.665(7)
Mo(11)-O(32)	1.871(8)	Mo(12)-O(26)	1.874(8)
Mo(11)-O(40)	1.891(8)	Mo(12)-O(37)	1.896(7)
Mo(11)-O(36)	1.947(7)	Mo(12)-O(29)	1.952(8)
Mo(11)-O(38)	1.988(9)	Mo(12)-O(40)	1.965(8)
Mo(11)-O(4)	2.440(6)	Mo(12)-O(4)	2.442(6)
P(1)-O(4)	1.526(6)	P(1)-O(1)	1.542(7)
P(1)-O(2)	1.535(7)	P(1)-O(3)	1.551(7)
Mo(13)-O(42)	1.696(8)	Mo(14)-O(45)	1.704(9)
Mo(13)-O(41)	1.699(9)	Mo(14)-O(44)	1.713(7)
Mo(13)-O(43)	1.923(6)	Mo(14)-O(43)	1.847(6)
Mo(13)-O(55A)	1.959(6)	Mo(14)-O(46)	2.055(6)
Mo(13)-N(2)	2.331(8)	Mo(14)-N(3)	2.335(9)
Mo(13)-N(1)	2.343(9)	Mo(14)-N(4)	2.339(8)
Mo(15)-O(49)	1.675(8)	Mo(16)-O(50)	1.703(7)
Mo(15)-O(47)	1.742(7)	Mo(16)-O(51)	1.735(8)
Mo(15)-O(46)	1.776(6)	Mo(16)-O(52)	1.798(6)

Mo(15)-O(48)	2.127(6)	Mo(16)-O(47)	2.244(7)
Mo(15)-N(6)	2.277(11)	Mo(16)-N(7)	2.257(8)
Mo(15)-N(5)	2.341(10)	Mo(16)-N(8)	2.320(8)
Mo(17)-O(53)	1.702(7)	Mo(18)-O(56)	1.678(8)
Mo(17)-O(48)	1.770(7)	Mo(18)-O(57)	1.724(9)
Mo(17)-O(54)	1.788(7)	Mo(18)-O(55)	1.813(6)
Mo(17)-O(52)	2.063(7)	Mo(18)-O(54)	2.085(6)
Mo(17)-N(9)	2.270(9)	Mo(18)-N(11)	2.314(9)
Mo(17)-N(10)	2.321(9)	Mo(18)-N(12)	2.346(8)
Mn(1)-O(51)	2.255(9)	Mn(1)-N(13)	2.046(2)
Mn(1)-N(13B)	2.518(2)	Mn(1)-N(14)	2.226(2)
Mn(1)-O(2W)	2.173(2)	Mn(1)-O(1WB)	2.558(2)
O(42)-Mo(13)-O(41)	105.4(4)	O(45)-Mo(14)-O(44)	106.2(4)
O(42)-Mo(13)-O(43)	98.9(3)	O(45)-Mo(14)-O(43)	102.2(4)
O(42)-Mo(13)-O(55A)	96.7(3)	O(45)-Mo(14)-O(46)	91.9(3)
O(42)-Mo(13)-N(2)	91.8(4)	O(45)-Mo(14)-N(3)	158.5(4)
O(42)-Mo(13)-N(1)	161.4(4)	O(45)-Mo(14)-N(4)	90.8(4)
O(49)-Mo(15)-O(47)	106.3(4)	O(50)-Mo(16)-O(51)	105.8(4)
O(49)-Mo(15)-O(46)	103.4(4)	O(50)-Mo(16)-O(52)	106.6(3)
O(49)-Mo(15)-O(48)	90.7(3)	O(50)-Mo(16)-O(47)	87.6(3)
O(49)-Mo(15)-N(6)	93.1(5)	O(50)-Mo(16)-N(7)	89.8(3)
O(49)-Mo(15)-N(5)	160.4(4)	O(50)-Mo(16)-N(8)	156.9(3)
O(53)-Mo(17)-O(48)	108.0(4)	O(56)-Mo(18)-O(57)	106.0(4)
O(53)-Mo(17)-O(54)	102.4(3)	O(56)-Mo(18)-O(55)	103.0(4)
O(53)-Mo(17)-O(52)	91.1(3)	O(56)-Mo(18)-O(54)	90.2(3)
O(53)-Mo(17)-N(9)	91.4(4)	O(56)-Mo(18)-N(11)	92.6(4)
O(53)-Mo(17)-N(10)	160.5(4)	O(56)-Mo(18)-N(12)	159.0(3)
N(13)-Mn(1)-N(14)	84.8(7)	N(13)-Mn(1)-N(13B)	67.3(8)
N(13)-Mn(1)-O(2W)	106.6(7)	N(13)-Mn(1)-O(1WB)	154.8(7)
N(13)-Mn(1)-O(51)	97.5(6)		

Symmetry transformations used to generate equivalent atoms: A: x+1/2, -y+1/2, z; B: -x+1, -y+1, z.

**Table S3** Selected H-Bonds in the crystal structure of **1**

X	H	Y	X-H	H...Y	X...Y	Symmetry
O1W		O51			3.387(2)	1-x, 1-y, z
C64	H64	O44	0.928(1)	2.418(7)	3.341(1)	1-x, 1/2-y, -1/2+z
C17	H17	O42	0.929(1)	2.453(8)	3.096(1)	3/2-x, y, 1/2+z
C14	H14	O41	0.931(1)	2.272(7)	3.124(1)	3/2-x, y, 1/2+z
C27	H27	O56	0.930(1)	2.344(7)	3.126(1)	1-x, 1/2-y, -1/2+z
C37	H37	O50	0.930(2)	2.673(7)	3.506(2)	1-x, 1/2-y, -1/2+z